Technical Notes

Pulsed Magnetoplasmadynamic Propulsion for Airbreathing Satellites in Very Low Earth Orbit

Joseph W. Zimmerman,* Rodney L. Burton,† Ryan T. Fox,‡
and David L. Carroll§
CU Aerospace, L.L.C., Champaign, Illinois 61822
and
Emil J. Broemmelsiek¶ and Edgar Choueiri**
Princeton University, Princeton, New Jersey 08544

https://doi.org/10.2514/1.B39990

Nomenclature

$\boldsymbol{B}$ = magnetic field, Tesla
E_o = pulse energy
F = pulse frequency
I_{bit} = impulse bit, $\text{mN} \cdot \text{s}$
I = current, A
$\boldsymbol{j}$ = current density, A/m^2
MPDT = magnetoplasmadynamic thruster
$\dot{m}$ = mass flow rate, kg/s
PFN = pulse forming network
QS = quasi-steady
T = thrust, N
TAPS = thermospheric airbreathing propulsion system
U = exhaust velocity, m/s and km/s
VLEO = very low earth orbit
V_o = PFN charging voltage, volts
η_t = thruster efficiency

I. Introduction

SATELLITES orbiting in Very Low Earth Orbit (VLEO) at altitudes of 150–250 km require continuous drag maintenance thrust from a solar electric propulsion system. Airbreathing versions of these satellites collect air at widely varying species compositions and densities that can vary by a factor of 30. The orbital velocity is nearly constant at $7800\ \text{m/s}$. Development of VLEO propulsion technology would enable the creation of small Earth imaging and atmospheric science satellites. Recent studies of airbreathing satellites include Allasio et al. [1], Herdrich et al. [2], and Giannetti et al. [3].

The coaxial pulsed self-field magnetoplasmadynamic thruster (MPDT) is being investigated for the VLEO satellite application. A pulsed system is inherently throttleable by varying the pulse frequency, allowing "drag-free" operations [1] during the wide density and drag excursions expected even in circular orbits. The MPDT discussed herein employs a $>10\ \text{kA}$, $370\ \mu\text{s}$ flat-top current pulse and a ms-long gas pulse. By using pulse energy in the kilojoule range, a megawatt arc discharge is created to generate the electron temperature, magnetic field and axial electric field required to rapidly dissociate, ionize, and accelerate ions to velocities exceeding $30\ \text{km/s}$ [4]. The high pulse power level provides complete dissociation and ionization at relatively low ion cost, as opposed to the partial ionization achieved by lower power propulsion systems with a steady-state discharge. Additionally, because accelerated ions are imbedded in a charge-neutral plasma, a gas-fed charge neutralizer is not required.

The quasi-steady (QS) current is provided by a capacitive pulse forming network [5], and the air propellant is provided by fast pulsed solenoid valves synchronized with the current pulse. The pulsed self-field MPDT has a long history [6] and was flown on-orbit in 1995–1996 [7]. The compact air-fed pulsed MPDT system discussed herein is referred to as the Thermosphere Airbreathing Propulsion System (TAPS). The developmental brassboard thruster head of TAPS is shown in Fig. 1. TAPS pulse energy operated as high as 688 J, delivered in $370\ \mu\text{s}$ at a QS pulse power of 1.8 MW.

TAPS is designed to be fueled on-orbit by a free molecular flow inlet that collects and feeds ram air into a flow compression system. An air pulse and simultaneous current pulse are fired every few seconds, ionizing and accelerating several 100 micrograms of air to a velocity of $25\text{–}50\ \text{km/s}$. Typically, the QS pulse thrust is 10–20 N for a sub-millisecond pulse. By discharging the bank energy E_o at a controllable pulse frequency $f < 1$ Hz, the average power is fE_o and the mean thrust can be throttled over the millinewton range as required by a small satellite at altitudes of 150–250 km. This thrust control method was first proved with a Teflon pulsed plasma thruster by the TIP/NOVA navigational satellite [8]. The TAPS MPD thrust acceleration mechanism has been amply demonstrated by extensive research on self-field electromagnetic discharges since the 1960s [6,9–14] along with in-space thruster operations [7].

This note briefly summarizes the compact, pulse forming network (PFN)-driven reverse polarity TAPS MPDT that was operated on two thrust stands for verification and validation using 0.5–1.8 MW pulses to generate exhaust velocities of $25\text{–}50\ \text{km/s}$. Hundreds of pulsed thruster tests ($V_o = 165$ to331 V) were performed in vacuum. Current and voltage waveforms were typical of expected stable MPDT behavior and were virtually identical for 100% N_2 and a 50:50 $\text{N}_2:\text{O}_2$ simulation of thermospheric orbital operations at $\sim$200 km altitude. Measurements of impulse bit $\boldsymbol{I}_{\text{bit}}$ ranged from 3.3 to $7.7\ \text{mN} \cdot \text{s}$ for voltages between 165–331 V. It is anticipated that geometry modifications, higher energy and extended pulse length will improve the impulse bit. Experiments showed no evidence of voltage "Onset" instability [15] for operating conditions of 331 V, 11 kA, and a quasi-steady mass flow rate of $0.5\ \text{g/s}$. Unique to this work are 1) the use of a reverse polarity MPDT and 2) test data with

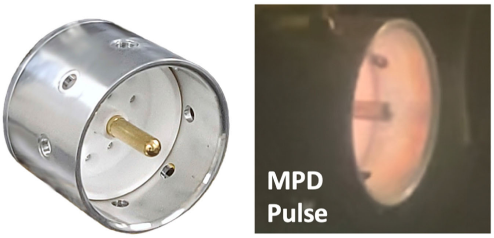

Fig. 1 **(Left) TAPS MPDT brassboard thruster head and (right) TAPS thruster plasma pulse.**

Received 22 January 2025; accepted for publication 15 August 2025; published online 16 September 2025.

[*] Director of Plasmadynamics. Associate Fellow AIAA.

[†] VP for Research. Associate Fellow AIAA.

[‡] Staff Engineer.

[§] President; carroll@cuaerospace.com. Fellow AIAA (Corresponding Author).

[¶] Research Staff, Electric Propulsion and Plasmadynamics Laboratory, Mechanical and Aerospace Engineering.

[**] Professor, Mechanical and Aerospace Engineering. Fellow AIAA.

a 50:50 $N_2:O_2$ gas mixture applicable to an ingested and recombined air mixture in VLEO.

II. TAPS MPDT Description

TAPS is a reverse polarity configuration with central anode and coaxial outer cathode, in contrast to the standard electrode polarity in previous MPDTs. Reverse polarity simplifies discharge ignition and was found to extend the exhaust velocity range, avoiding a plasma instability called Onset [14]. Electrode insulation is provided by a cylindrical Macor® anode insulator and a Macor® coaxial backplate insulator with gas injection ports. The radial distribution of injected mass flow varies as $1/r^2$ [15], matching the radial distribution in magnetic pressure [4]. Current is generated by a multisection, 14.8 mΩ pulse forming network (PFN) with capacitors and inductors and is directly connected to the electrodes by a coaxial line. Air is delivered by four fast-acting valves (FAVs) positioned around the circumference of the coaxial line, fed by a small volume plenum that is calibrated by measuring plenum pressure drop. A flow distribution plate distributes gas through nozzles during each thrust pulse. Four spark igniters located in the outer electrode are fired at low energy to initiate the current pulse just after the air pulse after charging the PFN to full energy. The PFN current pulse length is matched to the air pulse length, with the latter restricted by the minimum opening-closing time of the FAVs. TINA-TI circuit software (version 9.3) was applied to model the pulse waveforms of candidate PFN designs, and the simulated current and voltage waveforms generated were found to agree with measured waveforms at a capacitor charging voltage V_o of 320 V.

III. TAPS MPDT Testing

Thruster impulse performance was first tested in a 0.8 m^3 vacuum chamber using a compact Watts Pendulum thrust stand [16] to measure impulse bit at 0.5 g/s mass flow rate for a 370 μs current pulse. The anode diameter was 9 or 12 mm with a 30 mm exposed length, centered in a 72 mm diameter cathode of equal length. Nonrefractory electrode materials were employed to facilitate low-cost changes in electrode geometry. Figure 2 shows voltage and current waveforms for a 639 J MPDT pulse with 50:50 $N_2:O_2$ flow at a PFN charging voltage of 320 V. Thrust was initially computed from the measured I_{bit} divided by the QS pulse length of 0.370 μs. The thrust was cross-checked using the Maecker formula, Eq. (1) [17,18], and a QS current determined from the relatively stable QS voltage and the constant PFN impedance as determined by pulse length. The thrust values were found to be within ±5% of each other, with the Maecker formula generally slightly higher than the I_{bit} measurement:

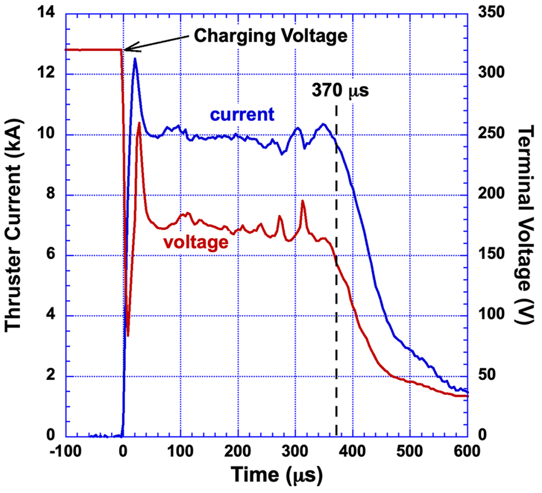

Fig. 2 TAPS 639 J (charging voltage 320 V) quasi-steady pulse waveforms for 50:50 $N_2:O_2$ mixture at 0.5 g/s with 9 mm anode and 72 mm cathode.

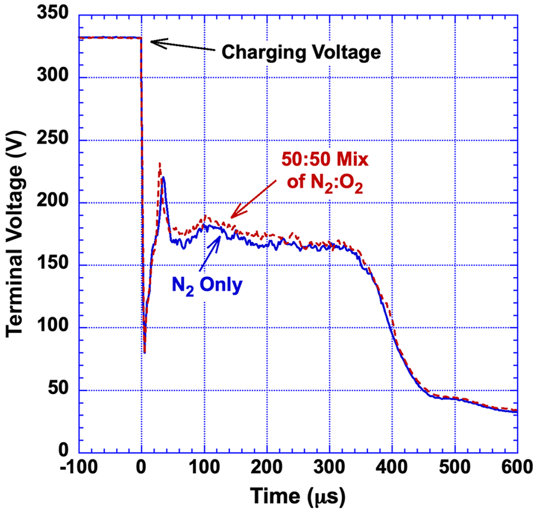

Fig. 3 Superimposed voltage waveforms comparing pure N_2 (blue) and 50:50 $N_2:O_2$ (red) mixtures at 684 J (charging voltage 331 V).

$$T = \frac{\mu_o}{4\pi} I^2 \left[\ln\left(\frac{r_{\mathrm{cathode}}}{r_{\mathrm{anode}}} \right) + c \right] \tag{1}$$

Figure 3 shows superimposed voltage waveforms for MPDT pulses with N_2 and 50:50 $N_2:O_2$ flow at a PFN charging voltage of 331 V. The pulse length and pulse voltage were consistent with design modeling using TINA-TI circuit software (version 9.3). The similarity of the waveforms demonstrate that the pulses are insensitive to variations in $N_2:O_2$ mixture ratio. This result is not surprising based on the similarities in atomic weight and ionization potential of the two diatomic species. The QS terminal voltage waveform is approximately half of the PFN charging voltage, as expected based on a PFN impedance of 14.8 mΩ and mean thruster impedance of 17.4 mΩ. The voltage waveforms display initial breakdown noise followed by low amplitude oscillations due to variations in impedance between 50–350 μs. The 50:50 $N_2:O_2$ mixture is representative of the expected plenum mixture at thermospheric altitudes, taking into consideration the recombination of atomic oxygen in a TAPS compression system. MPDT measurements for the two tested propellants at constant QS mass flow rate are listed in Table 1. Impulse bit varies from 3.0 to 7.7 mN · s, increasing with PFN charging voltage over a range of 165 to 331 V.

Waveform and impulse bit measurements were validated on a duplicate TAPS PFN and thruster system with N_2 propellant on a swinging gate thrust stand [19] in a much larger 20 m^3 dielectric vacuum chamber. The anode configuration for these tests was 9 mm diameter with a 30 mm exposed length, coaxial in a 72 mm diameter cathode of the same length. As with the first thrust test data set, refractory electrode materials were not employed. The character of the data measurements was similar between both test units in both the smaller and larger vacuum tanks. A significant transient voltage and current oscillation occurs at the initiation of the pulse. After an initial peak, the pulse current falls to 10 kA during the remainder of the pulse, then falls toward zero at 370 μs along with the voltage. After the initial transient, QS voltage is 170 V and impedance is 14.8 mΩ. Thrust stand impulse data were measured over a range of PFN charging voltages, holding the air pulse QS mass flow constant

Table 1 Averaged 50:50 $N_2:O_2$ and N_2 MPDT test cases taken in a 0.8 m^3 vacuum chamber

PFN charge voltage, V	QS mass flow, g/s	Impulse bIt, mN · s 1:1 $N_2:O_2$	Impulse bit, mN · s N_2
165	0.52	3.0	3.2
248	0.52	4.4	4.3
331	0.52	7.7	7.6

Data repeatability is ±3%.

(0.5 ± 2% g/s). The measured impulse bits, corrected by subtracting pre-pulse and post-pulse cold flow impulse, increase linearly from 4.7 mN · s at 244 V_o to 7.5 mN · s at 318 V_o. The scatter in the data is ±0.5 mN · s as expected based on the shot-to-shot repeatability of the current pulse. TAPS operated over a range of exhaust velocity U in the range of 23 to 52 km/s.

Calculations were performed to determine efficiency of the TAPS MPDT. The QS pulse length is constant as expected over a range of pulse current value of 7.5 to 10 kA corresponding to V_o from 165 to 331 V. The corresponding QS thrust efficiency is determined from the measured QS thrust, QS mass flow (0.51 g/s), voltage, and current:

$$\eta_t = \frac{T^2/2\dot{m}}{V_{\text{QS}} I_{\text{QS}}} \tag{2}$$

This efficiency was also examined using the thrust from the Maecker formula, Eq. (1). In this case the values of the thruster efficiency were found to be within ±10%, compared to the predicted error of ±11% (dominated by the error in ±5% error in the thrust), again with the Maecker formula generally higher than the I_{bit} measurement. The values presented in Fig. 4 are the more conservative values from the I_{bit} measurement. TAPS reached a thrust efficiency as high as 30% and operated over a range of exhaust velocity U in the range of 23 to 52 km/s.

The first set of impulse bit measurements with $N_2:O_2$ and N_2 in the 0.8 m^3 vacuum chamber at three PFN charging voltages with a 12 mm anode, were compared to the N_2 data in the 20 m^3 vacuum chamber at similar voltages with a 9 mm anode. The measured impulse bits from both facilities are in good agreement. The data from the small vacuum chamber for pure N_2 and the 1:1 $N_2:O_2$ mixture indicate that impulse performance is relatively independent of $N_2:O_2$ composition. Figure 4 shows QS thruster efficiency as a function of exhaust velocity U from both facilities compared to previous N_2 data taken with a classic central cathode MPDT [9] at current levels up to 30 kA, which enhanced thruster efficiency. Exhaust velocity in Fig. 4 is calculated from

$$U = I_{\text{bit}}/\dot{\text{m}}\text{t}_{\text{p}} \ [\text{N} \cdot \text{s}/(\text{kg/s} \cdot \text{s})]$$

We note that no Onset voltage instabilities were observed with the TAPS reverse polarity design in the range of exhaust velocities above 40 km/s, whereas classic polarity MPDT N_2 measurements with a central cathode were limited by observed Onset limits at 40 km/s [9], Fig. 4. Comparing the QS Onset parameter $I^2/\dot{m}$ for the two-test series shows Onset beginning at 225 kA^2/g/s for classic polarity [9] for nitrogen while no Onset is observed at 200 kA^2/g/s for TAPS data with reverse polarity [15].

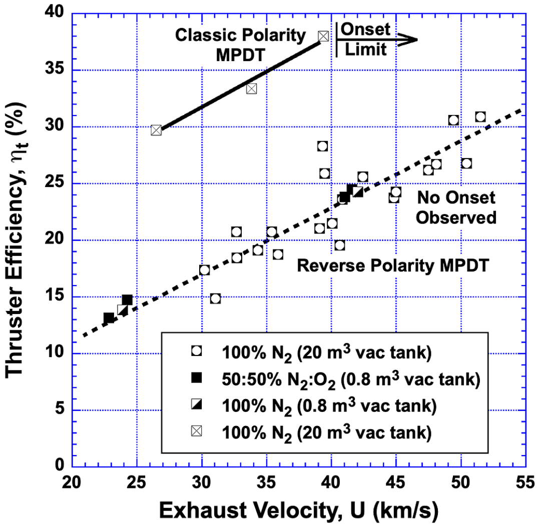

Fig. 4 TAPS reverse polarity MPDT thruster test results for N_2 and $N_2:O_2$ compared to test results from classic polarity MPDT for N_2 [9]. Note that onset limit for the classic polarity MPDT was 40 km/s, while the reverse polarity MPDT observed no Onset above 40 km/s.

IV. Conclusions

Thruster operation was verified and validated on two thrust stands using 0.5–1.8 MW pulses to generate high exhaust velocities of 25–50 km/s in $N_2:O_2$ and N_2. Waveforms typical of MPDTs with near flat top quasi-steady I(t) and V(t) traces were measured. Tests demonstrated $\boldsymbol{j} \times \boldsymbol{B}$ plasma acceleration ($T \sim I^2$) and a calculated pulsed thrust of >20 N. High QS exhaust velocity (~50 km/s) operation up to 10 kA of current was demonstrated. QS thrust efficiency was 23% at $U = 40$ km/s and exceeded 30% above 50 km/s. Measured Impulse-to-Energy ratio was 12 mN · s/kJ (12 mN/kW), very typical of MPDTs with low atomic mass propellants. No Onset instabilities were observed in the range of operation parameters that exceeded exhaust velocities observed in previous Onset limits [9]. Critical issues to be addressed in future TAPS MPDT work to increase thruster efficiency and lifetime include decreasing thruster impedance by scaling to higher and longer current levels by increasing PFN capacitance, introduction of optimized geometry refractory electrodes supported by detailed plasma magnetic and Langmuir probe measurements to address electrode erosion, parametric studies of injection and plasma flow conditions, improved matching of FAV and PFN discharge pulses, and repetitive life cycle vacuum testing of capacitors, inductors, FAVs, and igniters.

Acknowledgments

The application of the pulsed reverse-polarity MPDT to VLEO satellite propulsion was conceived by co-author Rodney Burton. This research was developed with funding from the Defense Advanced Research Projects Agency (DARPA) on Contract # N66001-22-C-4011. The authors wish to thank Stephen Forbes and Aaron Esposita for their guidance and support.

References

[1] Allasio, A., Anselmi, A., Catastini, G., Cesare, S., Dumontel, M., Saponara, M., Sechi, G., Tramutola, A., Vinai, B., and André, G., et al., "GOCE Mission: Design Phases and In-Flight Experiences," *215th Meeting, American Astronomical Society*, AAS Paper 2010-081, Springfield, VA, Jan. 2010.

[2] Herdrich, G., Papavramidis, K., Maier, P., J, Skalden, Hild, F., Beyer, J., Pfeiffer, M., Fugmann, M., Klinker, S., Fasoulas, S., et al., "System Design Study of a VLEO Satellite Platform Using the IRS RF Helicon-Based Plasma Thruster," *Acta Astronautica*, Vol. 215, Feb. 2024, pp. 245–259.
https://doi.org/10.1016/j.actaastro.2023.11.009

[3] Giannetti, V., Ferrato, E., and Andreussi, T., "On the Critical Parameters for Feasibility and Advantage of Air-Breathing Electric Propulsion Systems," *Acta Astronautica*, Vol. 220, July 2024, pp. 345–355.
https://doi.org/10.1016/j.actaastro.2024.04.042

[4] Burton, R. L., and Carroll, D. L., "Simplified Plasmadynamics Model of a Coaxial Self-Field Plasma Accelerator," *Journal of Propulsion and Power*, Vol. 39, No. 4, 2023, pp. 511–523.
https://doi.org/10.2514/1.B38923

[5] Glasoe, G. N., and Lebacqz, J. V., *Pulse Generators*, McGraw Hill Publ., New York, 1948, Chap. 6.

[6] Malliaris, A. C., John, R. R., Garrison, R. L., and Libby, D. R., "Performance of Quasi-Steady MPD Thrusters at High Powers," *AIAA Journal*, Vol. 10, No. 2, 1972, pp. 121–122.
https://doi.org/10.2514/3.50074

[7] Toki, K., Shimizu, Y., and Kuriki, K., "On-Orbit Demonstration of a Pulsed Self-Field Magnetoplasmadynamic Thruster System," *Journal of Propulsion and Power*, Vol. 16, No. 5, 2000, pp. 880–886.
https://doi.org/10.2514/2.5655

[8] Ebert, W. L., Kowal, S. J., and Sloan, R. F., "Operational NOVA Spacecraft Teflon Pulsed Plasma Thruster System," AIAA Paper 1989-2497, 1989.
https://doi.org/10.2514/6.1989-2497,

[9] Burton, R. L., Clark, K. E., and Jahn, R. G., "Measured Performance of a Megawatt MPD Thruster," *Journal of Spacecraft and Rockets*, Vol. 20, No. 3, 1983.
https://doi.org/10.2514/3.25596

[10] Uematsu, K., Morimoto, S., and Kuriki, K., "MPD Thruster Performance with Various Propellants," *Journal of Spacecraft and Rockets*, Vol. 22, No. 4, 1985, pp. 412–416.
https://doi.org/10.2514/3.25766

[11] Choueiri, E. Y., and Ziemer, J. K., "Quasi-Steady Magnetoplasmadynamic Thruster Performance Database," *Journal of Propulsion and Power*, Vol. 17, No. 4, 2001, pp. 967–976.
https://doi.org/10.2514/2.5857

[12] Ziemer, J. K., and Choueiri, E. Y., "Scaling Laws for Electromagnetic Pulsed Plasma Thrusters," *Plasma Sources Science and Technology*, Vol. 10, No. 3, 2001, pp. 395–394.
https://doi.org/10.1088/0963-0252/10/3/302

[13] Cooley, J. E., and Choueiri, E. Y., "Threshold Criteria for Under-Voltage Breakdown," *Journal of Applied Physics*, Vol. 103, No. 9, 2008, Paper 093305.
https://doi.org/10.1063/1.2913196

[14] Uribarri, L., and Choueiri, E. Y., "Creation of Onset Voltage Hash by Anode Spots in a Magnetoplasmadynamic Thruster," *Journal of Propulsion and Power*, Vol. 25, No. 4, 2009, pp. 949–957.
https://doi.org/10.2514/1.40847

[15] Burton, R. L., Carroll, D. L., and Zimmerman, J. W., Magnetoplasmadynamic Thruster with Reverse Polarity and Tailored Mass Flux, U.S. Patent # No. 12309909, 2025.

[16] Wilson, M., Bushman, S., and Burton, R. L., "A Compact Thrust Stand for Pulsed Plasma Thrusters," *25th International Electric Propulsion Conference*, Electric Rocket Propulsion Soc. Paper IEPC-97-122, Cleveland, OH, 1997, pp. 765–772.

[17] Maecker, H., "Plasmaströmungen in Lichtbögen Infolge Eigenmagnetischr Kompression," *Zeitschrift Fur Physik*, Vol. 141, Nos. 1–2, 1955, pp. 198–216.
https://doi.org/10.1007/BF01327300

[18] Jahn, R. G., *Physics of Electric Propulsion*, McGraw–Hill, New York, 1968, Chap. 8.

[19] Cubbin, E. A., Ziemer, J. K., Choueiri, E. Y., and Jahn, R. G., "Pulsed Thrust Measurements Using Laser Interferometry," *Review of Scientific Instruments*, Vol. 68, No. 6, 1997, pp. 2339–2346.
https://doi.org/10.1063/1.1148116

J. J. Szabo
Associate Editor